COMMUNICATIONS IN
DEVELOPMENT AND ASSEMBLING OF TEXTILE PRODUCTS

Combining protective clothes with human body models for finite element ballistic impact simulations

Matthias Boljen*, Marcin Jenerowicz[2], Steffen Bauer[3], Elmar Straßburger[4]

Ernst-Mach-Institute, EMI, Fraunhofer Institute for High-Speed Dynamics, Freiburg, Germany,
*Corresponding author *E-mail address:* matthias.boljen@emi.fraunhofer.de

INFO

CDAPT, ISSN 2701-939X
Peer reviewed article
2023, Vol. 4, No. 2, pp. 141-150
DOI 10.25367/cdatp.2022.4.p141-150
Received: 23 Februar 2023
Accepted: 24 March 2023
Available online: 07 May 2023

ABSTRACT

The ballistic deformation of an ultra-high-molecular-weight (UHMW) polyethylene (PE) composite has been subjected numerically to a multi-layered soft ballistic fabric package modelled upon the body contours of the Global Human Body Models Consortium (GHBMC) human body models M50-P and F05-P. The results of the clothing-body-interaction have been investigated and compared to the behavior of anthropomorphic surrogate models made from ballistic clay. For building the fabric model in donned shape, a single ply of woven fabric material has been converted upon the anthropomorphic body contour by subjecting it to a quasi-deep drawing process. After the fabric deformation, the shaped layer was duplicated 20 times and shifted outwards to build the fabric model, representing a multi-layered soft ballistic fabric package. The results of the ballistic impact simulation show that the response of the human body models (HBMs) is much more compliant than the behavior of the surrogate models. The deformation of the female HBM in terms of penetration depth and diameter of the affected impact region is slightly more severe than the deformation of the male counterpart with respect to identical impact conditions.

Keywords
clothes modeling,
finite element modeling,
human body models,
ballistic impact simulations,
injury assessment

1 Introduction

Finite element (FE) human body models (HBM) are intensively being applied to crash and impact simulations in automotive applications [1−4]. Though these models have already been validated against a multitude of load cases, their use in defense applications to study kinetic threats against the human body is rather limited. One of the reasons is the challenge to model flexible clothes as well as protective components in worn shape, i.e. directly on the human body. Though many constitutive models dedicated

to fabric materials are available for various applications [5−9], only few attempts have been made to use them in clothing models on HBM directly. Moreover, involving HBM in crash and impact simulations typically requires multi-staged modeling processes, i.e. not only the actual load case, but also body posture and the integration of gravitational effects might require additional modelling efforts.

Ishimaru et al. developed an FE model to dress knitted fabrics to an HBM, sewed the pieces together, and calculated the resulting clothing pressure and thereby introduced a method to design virtually tight-fitting clothing [10]. Long et al. analyzed draping effects of single layer clothes on the human body due to gravitational effects [11]. Aggromito et al. investigated how the distribution of personal equipment on the body of military helicopter pilots affects the injury potential during a crash [12]. For this study, the primary survival gear carrier sitting on top of the flight suit and the body armor of the upper torso were modeled. The discretization of the carrier was based on the given mesh of the torso. Brolin and Wass used an HBM to investigate dangerous accidents in equestrian sports [13]. The protective capacity of a safety vest with respect to falls, kicks and horse trample had been assessed. Again, the mesh of the vest model had been based on the external torso geometry. Li et al. applied the modeling approach of Brolin and Wass to a study where protective vests could reduce the injury risk of aged people when falling down accidentally [14]. Again, the bulk mesh had been constructed by offsetting the nodes of the skin. Grassi et al. introduced the concept of a belted safety jacket for powered-two wheelers, and by design of experiment, they verified the effectiveness of such a jacket in collisions with other vehicles and the potential to reduce the injury risk of the rider [15].

Klein et al. presented a modeling method to drag simple pieces of cloth from a 2D shape into the 3D shape defined by the body surface of the wearing person [16]. The method resembles a deep drawing process with a dynamically evolving stamp geometry, whereas the original body surface is continuously being restored after having been scaled down to a minimum in the first place (Fig. 1). While the method provides an easy means to drape flexible objects to arbitrary contours, it is limited to simple pieces of cloth, since sewing patterns cannot be considered. More complex clothes, e.g. long sleeve shirts, finger gloves, especially when being combined with HBM postures describing active movements with wrinkled extremities or body parts still cannot be captured with this approach.

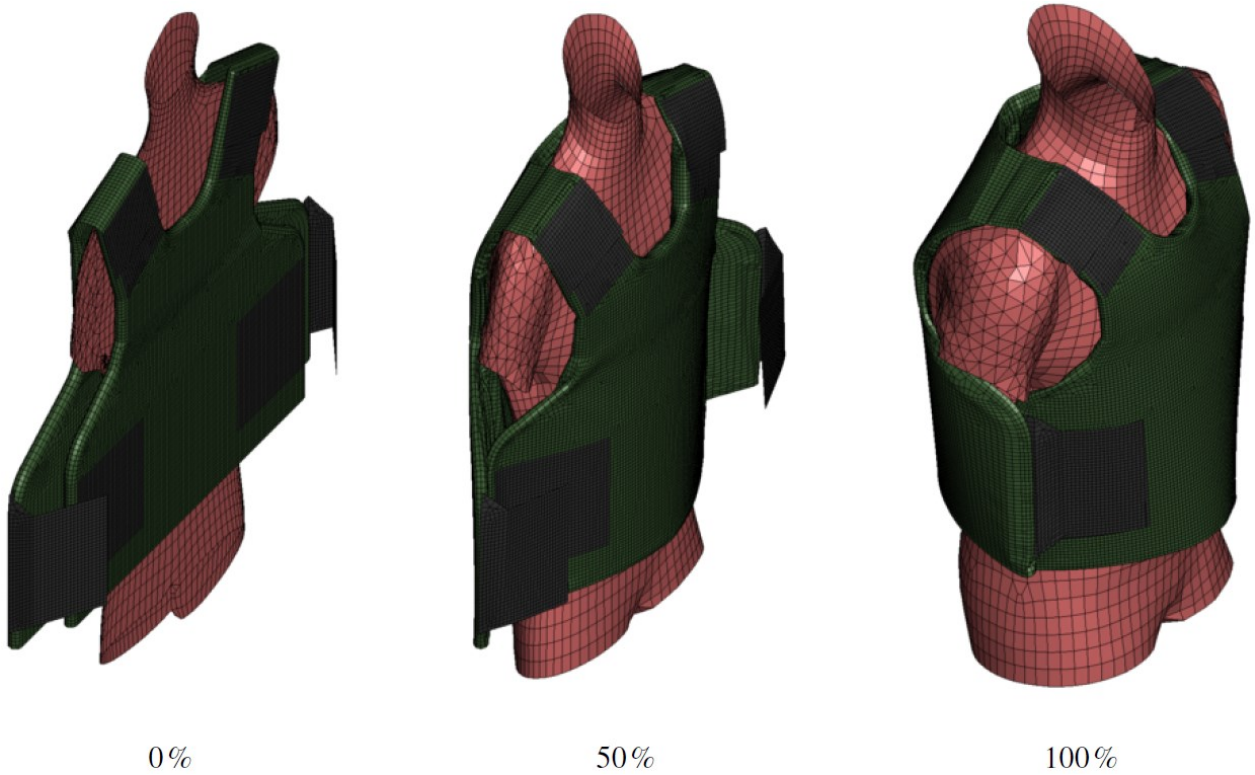

Fig. 1 Forming process of a finite element vest model from 2D planar to 3D donned shape at various stages with the body contour of the GHBMC M50 expanding from the interior of the vest. From [16], originally published under a CC-BY-NC license.

(a) *(b)*

Fig. 2 (a) Multi-layered fabric pack of soft-ballistic vest; (b) 40 layers of aramid woven fabric.

Nevertheless, the proposed method can be modified and applied in an alternative manner, namely by inversely pressing a flexible, planar object from the outside down onto the HBM contour. In this study, this procedure will be investigated for a multi-layered fabric pack of a soft-ballistic package. Fig. 2 illustrates the soft ballistic package that is going to be applied to the midsize male and small female GHBMC models used in this study.

2 Method

A ballistic deformation will be applied to this soft-ballistic package arising from the impact of a 7.62 mm × 51 AP projectile on a hard-ballistic plate made of Silicon carbide (SiC) and an ultra-high-molecular-weight (UHMW) polyethylene (PE) composite. The impact energy transferred into the fabric package and into the deformation of the bodies is analyzed and compared to the behavior of Roma Plastilina No. 1 which is used in standard test regulations [17,18]. This section describes the setup of the simulation models, which requires the following steps:

- the modeling of the soft ballistic fabric package in donned shape,
- the torso surrogate modeling based upon the HBM geometries,
- the modeling of the ballistic impact conditions.

2.1 Modeling of clothes in worn shape

The soft ballistic package shown in Fig. 2 consists of 3 fabric packages. These packages hold 13, 14, and 13 single plies, respectively. The plies are oriented in 0°/90° and ±45° direction in an alternate fashion, whereas each ply has a thickness of 0.28 mm. The plies are tied together along the boundary. Material parameters are taken from Ivanov and Tabiei [6]. In contrast to forming the whole vest including all layers in one step [16], only the innermost fabric layer has been subjected to the forming algorithm. The virtual punch is created by an upscaled duplicate of the body surface of the GHBMC M50, which represents a 50th percentile male person (height 175 cm, mass 79 kg). This implementation opens a gap between the punch and the body surface of approximately 350 mm in which the undeformed fabric ply is located. The material points of the punch are then translated back close to their original position on the body surface. The fabric ply consisting of roughly 12,500 quadrilateral shell elements is thereby forced to the shape of the body surface (Fig. 3).

(a) (b) (c) (d)

Fig. 3 (a) Setup for forming the innermost fabric layer on GHBMC M50; Intermediate configurations after completion of (b) 60%; (c) 80% and (d) 95% displacement.

(a) (b) (c) (d)

Fig. 4 (a) Setup for forming the innermost fabric layer on GHBMC F05; Intermediate configurations after completion of (b) 60%; (c) 80% and (d) 95% displacement.

The procedure has also been applied to the body contour of the GHBMC F05, which represents a 5th percentile female person (height 150 cm, weight 48 kg). The size of the fabric layer has been reduced by 10% in vertical and horizontal direction to account for the reduced body size. The punch was again scaled up to encompass a distance of 350 mm from the body surface and scaled back towards the body to almost the initial configuration (Fig. 4).

To reduce model complexity, each layer in the model has been assigned to two integration points in thickness direction to represent two fabric plies sticking on top of each other. After the forming of the innermost layer were completed, it has been duplicated 20 times and shifted outwards to represent the complete soft ballistic package.

2.2 Torso surrogates modeling

In order to compare the response of the GHBMC models to current testing procedures, torso surrogate models have been built based upon the skin contour of the human body models. The Altair HyperMesh preprocessor has been used to import the shell elements representing the skin of the neck, torso and pelvis of each model. The body contour has been approximated by drawing polylines and creating surfaces based upon the existing nodal coordinates. From merging the surface geometries, the interior body volume could be reconstructed.

Table 1. Data of torso surrogates.

Target	Mass (kg)	Volume (L)	Surface (cm^2)	Nodes (k)	Elements (k)
M50 GHBMC	41.7	41.4	555.0	842	1,429
M50 Clay Surrogate	56.9	37.2	554.0	32	158
F05 GHBMC	26.8	29.3	507.4	676	1,363
F05 Clay Surrogate	44.5	29.1	484.1	28	136

(a) *(b)* *(c)* *(d)*

Fig. 5 Body models used in this study: (a) GHBMC M50-P; (b) M50 torso surrogate based upon M50-P; (c) GHBMC F05-P; (d) F05 torso surrogate based upon F05-P.

Finally, the interior volume was discretized using 4-node tetrahedron elements. The characteristic element size was chosen to be approximately the same as in the original mesh. The solid elements were associated with ballistic clay material properties derived by Buchely et al. [19]. Table 1 compares basic characteristics of the male and female body models with their surrogate counterparts. Fig. 5 shows the corresponding models.

2.3 Modeling of ballistic impact conditions

The interaction between the projectile and the materials used for the SAPI (small-arms projectile insert) has been investigated experimentally in an isolated setup. SAPI typically consist of a ceramic layer and a composite backing material. In this study, a Silicon carbide (3M SiC T) ceramic of 9 mm thickness and a backing material of UHMW polyethylene (DSM Dyneema™) of 10 mm thickness have been tested (total areal weight 38 kg/m^2). The assembly was struck by a 7.62 mm × 51 AP projectile of mass 8.3 g travelling at 930 m/s. In most experiments, the above setup proved to defeat the threat successfully. Nevertheless, the bullet and the ceramic layer sustained heavy fragmentation. The deformation of the UHMW polyethylene composite is significant and was successfully reproduced in an AUTODYN simulation (Fig. 6). The final layer of the assembly is not penetrated and reaches a maximum local displacement of 30.4 mm at 0.2 ms after impact. The displacement-time-history of all nodes of the outer UHMW polyethylene layer has been extracted and converted into a kinematic constraint, so that the effective deformation of the layer can be reproduced and exerted onto the soft ballistic fabric package modelled previously (Fig. 3 and Fig. 4). The point of maximum displacement is located close the proximal end of the sternum (M50: 124 cm above the ground, F05: 108 cm above the ground).

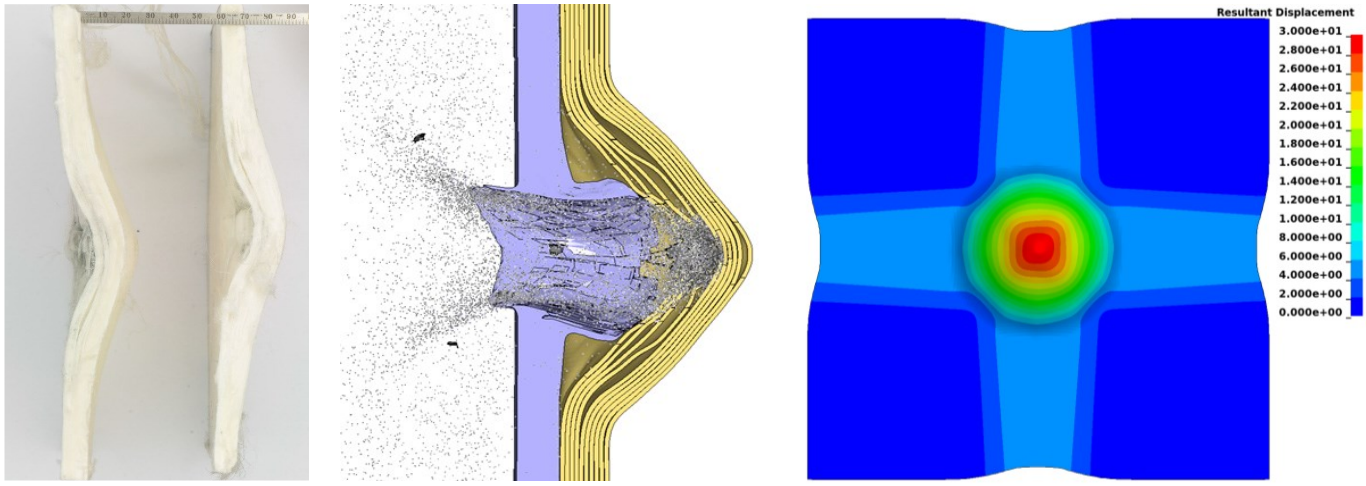

(a) (b) (c)

Fig. 6 UHMW-PE backing impacted by 7.62 mm × 51 AP ammunition: (a) deformed UHMW-PE specimen from impact experiments; (b) AUTODYN simulation; (c) extracted displacements of the outside polyethylene layer 0.2 ms after impact.

Table 2. Comparison of ballistic deformation characteristics against the selected threat in terms of penetration depth, indention diameter and time of maximum penetration.

Target	Time (ms)	Penetration (mm)	Diameter (mm)
M50 GHBMC (version 5.3.3)	1.81	48.2	146.6
M50 Clay Surrogate	0.38	13.8	73.2
F05 GHBMC (version 5.3.3)	1.90	54.3	164.0
F05 Clay Surrogate	0.38	13.7	71.1

3 Results

This section holds the results of the impact simulations for the select threat against the GHBMC human body models M50 and F05 and their corresponding torso surrogate models. The results were evaluated in order to find answers to the questions:

- Do the HBMs behave similarly in terms of penetration depth and diameter of the body region directly affected by the projectile impact?
- Are there differences regarding male and female anthropometries, and if true, how significant are these differences quantitatively?

3.1 Penetration depth and diameter

The impacted surfaces of the HBM and the torso surrogate models have been investigated in order to find the point of the maximum displacement and the diameter of the affected area. As a threshold, all nodes were selected whose total displacement exceed 20% of the maximum displacement. The results are summarized in Tab. 2. It becomes evident that the HBMs react far more compliant than the torso surrogate models. The maximum indention of the deformation is reached after 1.81 ms and 1.90 ms for the M50 and the F05 human body model, respectively, in contrast to 0.38 ms for both torso surrogate models.

- The deformation of the M50 human body model is characterized by a penetration depth of 48.2 mm and a diameter of 146.6 mm, which is 3.5 times and 2.0 times the extent compared to the deformation of the male torso surrogate (Fig. 7).
- The deformation of the F05 human model is characterized by a penetration depth of 54.3 mm and a diameter of 164.0 mm, which is 4.0 times and 2.3 times the extent compared to the deformation of the female torso surrogate (Fig. 8).

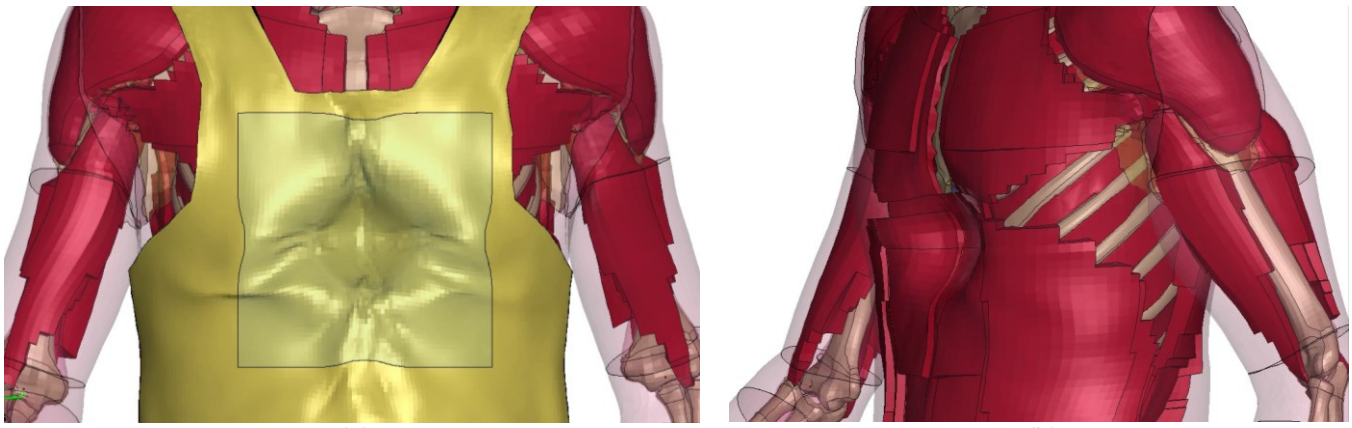

(a) (b)

Fig. 7 (a) Fabric pack on the GHBMC M50 chest at 1 ms; (b) back face deformation of the HBM.

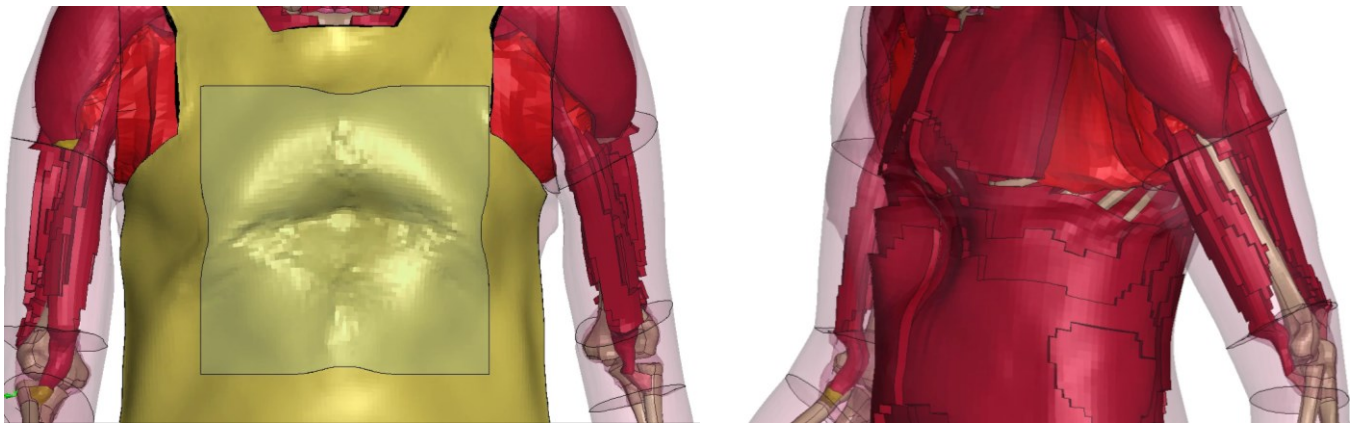

(a) (b)

Fig. 8 (a) Fabric pack on the GHBMC F05 chest at 1 ms; (b) back face deformation of the HBM.

3.2 Torso deformation history

To obtain more detailed information about the deformation at the impact location, the location of the nodes on the surface have been plotted in the body's transversal plane at various points of time after impact. Fig. 9 shows the deformation of the male sections for the HBM and the M50 torso surrogate model, whereas Fig. 10 shows the deformation of the female sections for the HBM and the F05 torso surrogate model. In both cases, the deformation of the ballistic clay is by far less severe than the deformation of the HBM, where approximately 80% of the final deformation is completed in the first 0.6 ms after impact.

4 Conclusions

The ballistic performance of 9 mm Silicon carbide and 10 mm UHMW polyethylene have been investigated against the impact of a 7.62 mm × 51 AP projectile. The resulting ballistic deformation of the composite material has been subjected to a multi-layered soft ballistic fabric package. The effect of the fabric deformation upon the GHBMC human body models M50 and F05 as well as corresponding solid replica made from ballistic clay have been evaluated. The following conclusions can be drawn:

- Significant deviations between the torso surrogates and HBM were detected for both models, the midsize male and the small female. The HBM were far more compliant in terms of penetration depth and diameter of the affected tissue in the region of impact. Kneubühl implies that ballistic materials like clay or gelatin generally react stiffer than human tissue and that these materials are primarily used to produce good repeatability and easy-to-measure plastic deformation, but not intend to reproduce the exact deformation characteristics of human tissue [20]. Alternative HBMs

need to be taken into consideration, e.g. the HUByx model (Hermaphrodite Universal Biomechanical YX model) could be used to compare the results to the male GHBMC model [4].

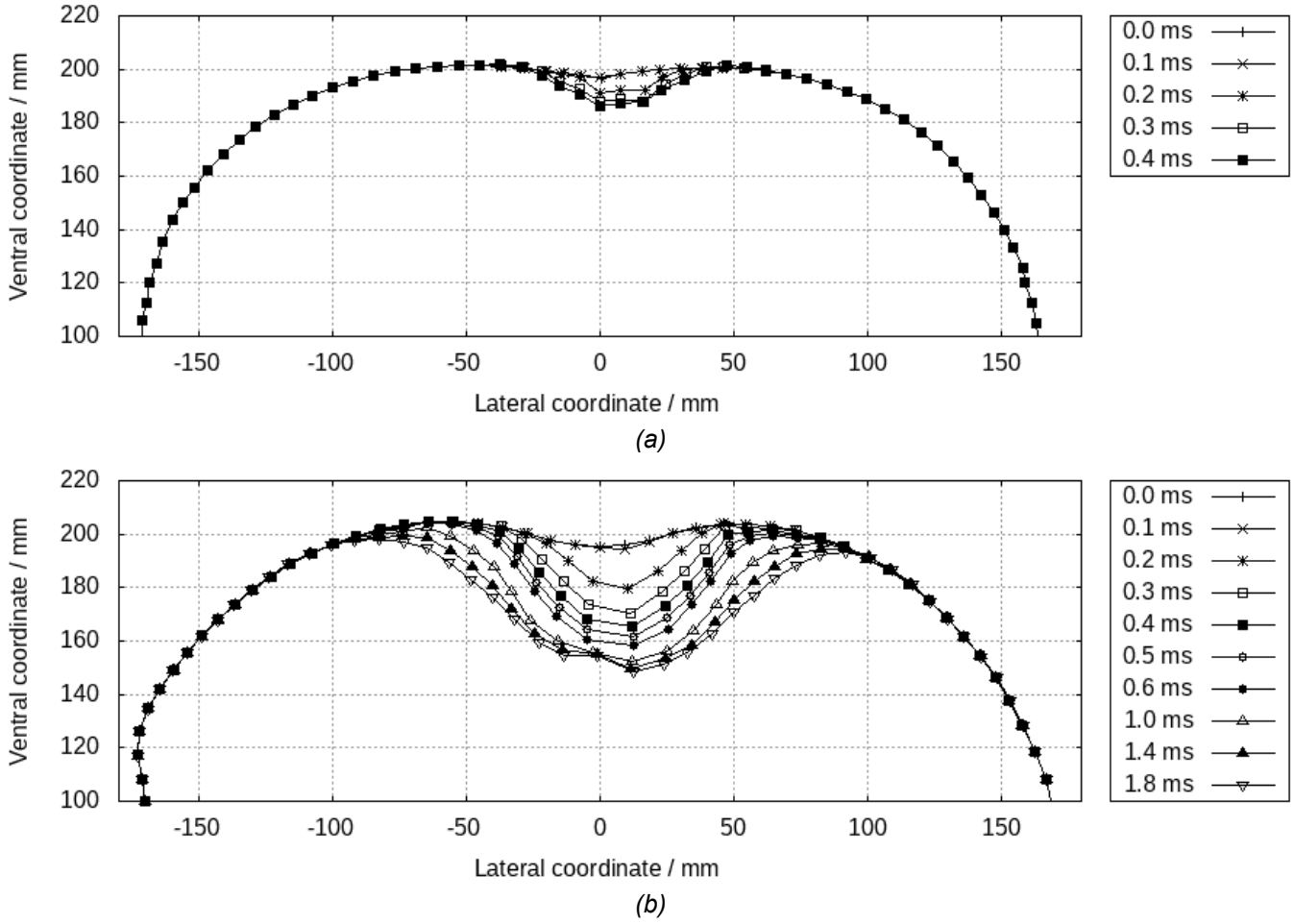

Fig. 9 Deformation contour plots over time: (a) Male 50 percentile torso surrogate; (b) GHBMC M50-P.

- The HBM representing the small female shows more severe deformations than the male HBM (relative increase of 12% in penetration depth and diameter of impacted area). This finding seems to confirm an earlier study of Bir and Viano [21]. The differences between the male and female torso surrogate models are negligible which indicates that the responses deduced by the male and female HBM cannot be related to the body geometry, but to different constitutive properties. Since ballistic clay cannot account for this aspect, it should be considered in future developments.
- This study successfully combines a ballistic load on both, a soft ballistic package and a HBM in a single FE simulation. Thus, a method is established to further assess potential injuries due to the deformation of internal organs, i.e. heart, lungs, spleen and the ribs. The results need to be compared to similar studies and evaluated against available ballistic injury criteria [21,22].
- Further studies on the influence of different fabric materials and textile architectures are needed. The influence of seam lines, different ply orientations and interlaminar friction can be investigated and compared to this reference model. For the female person, specific cutting patterns should be considered in order to improve the fit of the vest on the body.
- Experimental data is needed with regard to innovative anthropomorphic test devices. The latest CTS PRIMUS dummy offers calibration measures to account for ballistic impact conditions [23]. High-speed visual recordings or dynamic X-ray testing of the dummy interior would be helpful to measure displacements of dummy components, like rib structures, organ surrogates as long as the requirement for anti-penetrating ballistic conditions is met.

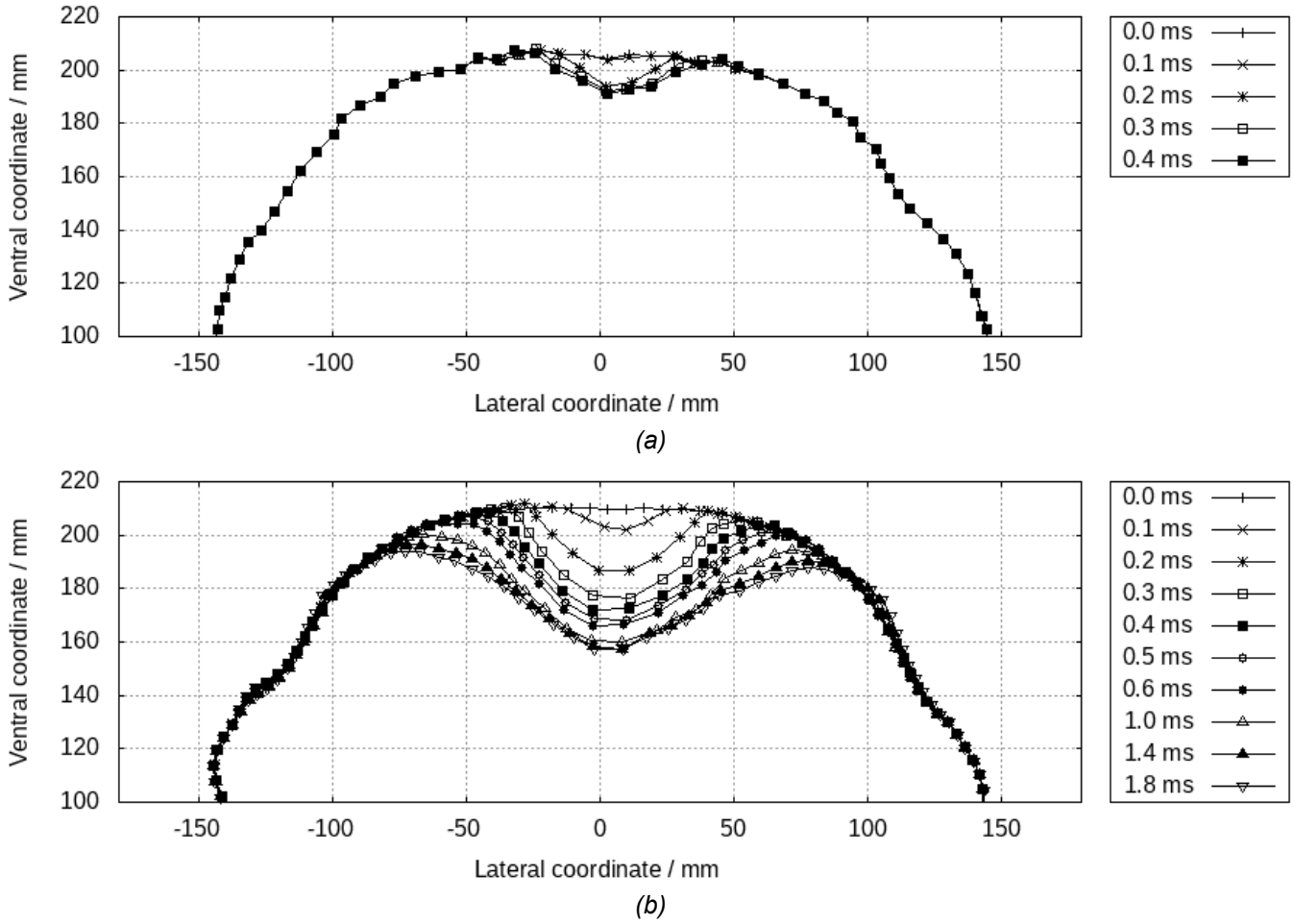

Fig. 10 Deformation contour plots over time: (a) Female 5 percentile torso surrogate; (b) GHBMC F05-P.

Author Contributions

M. Boljen: conceptualization, methodology, software, writing – original draft preparation, visualization; M. Jenerowicz: investigation, resources; writing – review and editing; S. Bauer: investigation, resources, writing – review and editing; E. Straßburger: supervision, project administration. All authors have read and agreed to the published version of the manuscript.

Acknowledgements

We would like to express our appreciation to the Federal Office of Bundeswehr Equipment, Information Technology and In-Service Support (BAAINBw) as well as Bundeswehr Technical Center for Weapons and Ammunition (WTD 91-450) for funding this work.

Conflicts of Interest

The authors declare no conflict of interest.

References

1. Untaroiu, C. D.; Pak, W.; Meng, Y.; Schap, J.; Koya, B.; Gayzik, S.: A Finite Element Model of a Midsize Male for Simulating Pedestrian Accidents, *Journal of Biomechanical Engineering* **2016**, *140*(1), 011003. DOI: 10.1115/1.4037854.
2. Grindle, D.; Pak, W.; Guleyupoglu, B.; Koya, B.; Gayzik, S.; Song, E.; Untaroiu, C., A detailed finite element model of a mid-sized male for the investigation of traffic pedestrian accidents. *Proceedings of the Institution of Mechanical Engineers, Part H: Journal of Engineering in Medicine* **2021**, *235*(3), 300–313. DOI: 10.1177/0954411920976223.

3. Iwamoto, M.; Nakahira, Y.: Development and validation of the total HUman model for safety (THUMS) version 5 containing multiple 1D muscles for estimating occupant motions with muscle activation during side impacts. *Stapp Car Crash Journal* **2015**, *59*, 53–90, DOI: 10.4271/2015-22-0003.
4. Roth, S.; Torres, F.; Feuerstein, P.; Thoral-Pierre, K.: Anthropometric dependence of the response of a thorax FE model under high speed loading: validation and real-world accident replication. *Computer Methods and Programs in Biomedicine* **2013**, *110*(2), 160–70. DOI: 10.1016/j.cmpb.2012.11.004.
5. King, M. J.: A Continuum Constitutive Model for the Mechanical Behavior of Woven Fabrics Including Slip and Failure. PhD thesis, Massachusetts Institute of Technology, Cambridge, MA, 2006.
6. Ivanov, I.; Tabiei, A.: Loosely woven fabric model with viscoelastic crimped fibers for ballistic impact simulations. *International Journal for Numerical Methods in Engineering* **2004**, *61*, 1565–1583. DOI: 10.1002/nme.1113.
7. Shahkarami, A.; Vaziri, R.: A Continuum Shell Finite Element Model for Impact Simulation of Woven Fabrics. *Intern. Journal of Impact Engineering* **2007**, *34*(1), 104–119, DOI: 10.1016/j.ijimpeng.2006.06.010.
8. Ballhause, D.: Diskrete Modellierung des Verformungs- und Versagensverhaltens von Gewebemembranen. PhD thesis, University Stuttgart, 2007.
9. Boljen, M., Hiermaier, S.: Continuum constitutive modeling of woven fabrics, *European Physical Journal Special Topics* **2012**, *206*, 149–161. DOI: 10.1140/epjst/e2012-01596-0.
10. Ishimaru, S.; Isogai, Y.; Matsui, M.; Furuichi, K.; Nonomura, C.; Yokoyama, A.: Prediction method for clothing pressure distribution by the numerical approach: attention to deformation by the extension of knitted fabric. *Textile Research Journal* **2011**, *81*(18), 1851–1870. DOI: 10.1177/0040517511410106.
11. Long, J.: Simulation-based assessment for construction helmets and clothing. Master thesis, Texas Tech University, Lubbock, TX, 2012.
12. Aggromito, D.; Thomson, R.; Wang, J.; Chhor, A.; Chen, B.; Yan, W.: Effect of body-borne equipment on injury of military pilots and aircrew during a simulated helicopter crash. *International Journal of Industrial Ergonomics* **2015**, *50*, 130–142. DOI: 10.1016/j.ergon.2015.07.001.
13. Brolin, K. & Wass, J.: Explicit Finite Element Methods for Equestrian Applications. *Procedia Engineering* **2016**, *147*, 275–280. DOI: 10.1016/j.proeng.2016.06.277.
14. Li, J.; Duanduan, C.; Tang, X.; Li, H.: On the protective capacity of a safety vest for the thoracic injury caused by falling down. *BioMedical Engineering OnLine* **2017**, *18*, 40. DOI: 10.1186/s12938-019-0652-3.
15. Grassi, A.; Barbani, D.; Baldanzini, N.; Barbieri, R.; Pierini, M.: Belted Safety Jacket: a new concept in Powered Two-Wheeler passive safety. *Procedia Structural Integrity* **2018**, *8*, 573–593. DOI: 10.1016/j.prostr.2017.12.057.
16. Klein, H.; Jenerowicz, M.; Trube, N.; Boljen, M.: How to Combine 3D Textile Modeling with Latest FE Human Body Models. *Advances in Transdisciplinary Engineering* **2020**, *11*, 166–177. DOI: 10.3233/ATDE200022.
17. NIJ Standard 0101.06. *Ballistic Resistance of Body Armor,* National Institute of Justice, U.S. Department of Justice, Washington, DC, July 2008.
18. ASTM E3004-22: Standard Specification for Preparation and Verification of Clay Blocks Used in Ballistic-Resistance Testing of Torso Body Armor. DOI: 10.1520/E3004-22.
19. Buchely, M. F.; Maranon, A.; Silberschmidt, V. V.: Material Model for Modeling Clay at High Strain Rates. *International Journal of Impact Engineering* **2016**, *90*, 1–11. DOI: 10.1016/j.ijimpeng.2015.11.005.
20. Kneubühl, B.; Ballistic Protection, 2002. Vereinigung der Prüfstellen für angriffshemmende Materialien und Konstruktionen (VPAM). https://www.vpam.eu/wp-content/uploads/2020/06/Ballistic-protection.pdf (accessed 2023/03/20).
21. Bir, C; Viano, D. C.: Design and Injury Assessment Criteria for Blunt Ballistic Impacts, *The Journal of Trauma: Injury, Infection, and Critical Care* **2004**, *57*, 1218–1224. DOI: 10.1097/01.ta.0000114066.77967.de.
22. Bir, C.; Viano, D. C.; King, A.: Development of biomechanical response corridors of the thorax to blunt ballistic impacts, *Journal of Biomechanics* **2004***, 37*, 73–79. DOI: 10.1016/S0021-9290(03)00238-0.
23. Schäuble, A.; Weyde, M.: Biomechanical Validation of a New Biofidelic Dummy. NHTSA 26th ESV, 2019.